Available online at www.sciencedirect.com
SCIENCE DIRECT®
Surface and Coatings Technology 177–178 (2004) 682–687
SURFACE & COATINGS TECHNOLOGY
www.elsevier.com/locate/surfcoat

Generation of electron-beam produced plasmas and applications to surface modification

D. Leonhardt*, C. Muratore[1], S.G. Walton, D.D. Blackwell[2], R.F. Fernsler, R.A. Meger

Naval Research Laboratory, Plasma Physics Division, 4555 Overlook Ave SW, Washington, DC 20375, USA

Abstract

NRL has developed a number of hollow cathodes to generate sheets of electrons culminating in a 'Large Area Plasma Processing System' (LAPPS) based on the electron-beam ionization process. Beam ionization is fairly independent of gas composition and produces low temperature plasma electrons (<0.5 eV in molecular gases) in high densities (10^9–10^{12} cm^{-3}). The present system consists of a pulsed planar plasma distribution generated by a magnetically collimated sheet of 2 kV electrons (<1 mA/cm^2) injected into a neutral background of processing gases (oxygen, nitrogen, sulfur hexafluoride, argon). Operating pressures range from 2–13 Pa with 150–165 Gauss magnetic fields for a highly localized plasma density of $\sim 10^{11}$ cm^{-3}. This plasma source demonstrated anisotropic removal rates of polymeric (photoresist) material and silicon with O_2 and $Ar/O_2/SF_6$ mixtures, respectively. In pure nitrogen, this same source showed a surface nitriding rate of ~ 1 $\mu m/h$ of plasma exposure time on austenitic stainless steel at 400 °C. Time-resolved in situ plasma diagnostics (Langmuir probes and mass spectrometry) of these pulsed plasmas are also shown to illustrate the general plasma characteristics.
© 2003 Elsevier B.V. All rights reserved.

Keywords: Large area plasmas; Plasma processing; Electron-beam ionization; Materials processing

1. Introduction

Electron beam (e-beam) ionization has been shown to be both efficient at producing plasma and scalable to large area (square meters). Fernsler [1], Manheimer et al. [2] have discussed the detailed physics behind the plasma production mechanisms, which agree with experimental in situ measurements [3,4]. More recently, a broader view of e-beam produced plasmas was presented [5] to illustrate both the fundamental aspects and the range of plasma source configurations being investigated for various applications. This paper reports on the recent experimental progress of the applications that are being pursued for materials' surface modification, with an additional emphasis on the plasma source construction.

Conventional discharges directly heat electrons with externally applied fields to ionize the gas, which results in a significant loss of input power to low-energy gas excitation processes rather than ionization or dissociation. Additionally, plasmas sustained by heated electrons have electron temperatures of multiple electron volts, which generally translates to a plasma environment of high plasma potentials (>10 V), sheath drops and ion isotropy at surfaces. When a high energy beam of electrons passes through a gas, its dominant energy loss process is ionization of the gas followed by dissociation and finally excitation. Secondary electrons are created over a wide energy spectrum but cool rapidly through collisions with the background gas before being destroyed and thus the plasma electron temperature is low. Moreover, the direct ionization mechanism makes the plasma production process extremely efficient when compared to conventional plasma discharges. These attributes make e-beam generated plasmas ideal for materials applications from surface activation of fragile polymer substrates to high energy reactive ion etching of hard semiconductor materials.

2. Experimental

2.1. Hollow cathode design for electron beam generation

For all experiments discussed in this paper, a plasma 'layer' was used. A sheet-beam of high energy electrons

*Corresponding author. Tel.: +1-202-767-7532; fax: +1-202-767-3553.
E-mail address: darrin@ccs.nrl.navy.mil (D. Leonhardt).
[1] ASEE/NRL Postdoctoral Research Associate.
[2] SFA, Inc., Largo, MD.

0257-8972/04/$ - see front matter © 2003 Elsevier B.V. All rights reserved.
doi:10.1016/j.surfcoat.2003.08.007

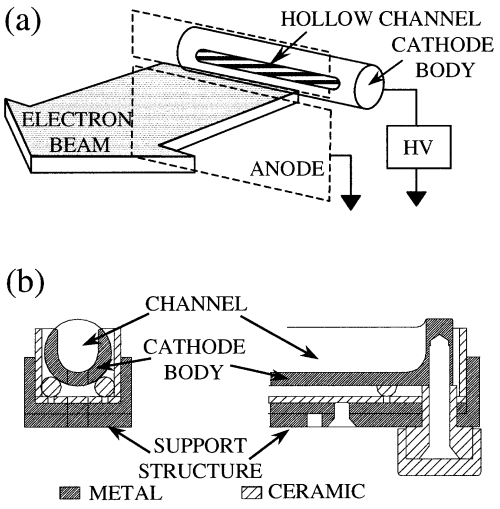

Fig. 1. (a) Geometric layout of pulsed e-beam plasma system and (b) cross sectional detail of linear hollow cathode construction.

was produced by a linear hollow cathode to generate the plasma layer. The hollow cathode was operated with a -2 kV, 2 ms pulse at 10–20% duty factors, with typical currents of 50–100 mA/pulse, depending on the application. Fig. 1a shows the basic geometry for e-beam plasma production in these experiments, and Fig. 1b provides a detail of the linear hollow cathode construction. The electron beam (a fraction of the cathode operating current) was accelerated out from the hollow channel and skimmed by a (grounded) stainless steel anode to set the beam's geometric shape. The anode, made from 0.2-cm (1/16 inch) thick plate, was located 5–8 cm in front of the cathode and provided a 25×1 cm slot. An axial magnetic field provided by either Helmholtz coils or a segmented solenoid arrangement kept the beam profile planar.

The views of the cathode assembly in Fig. 1b show the cathode, insulating material and the grounded support structure. All metal parts were made from 316 stainless steel while all insulators were made from machinable ceramic (Macor® or boron nitride) [6]. Standard 1.6 cm (5/8 inch) diameter metal rod stock was used for the cathode body. The hollow channel was cut with a 1.0 cm (3/8 inch) ball mill, approximately 1.3 cm (1/2 inch) deep along the central portion of the rod, then polished to a mirror-like finish. The metal support structure consisted of standard square U-channel stock with minor modifications and was grounded to the vacuum chamber. Electrical connections and mechanical support of the cathode were made with ceramic shoulder washers and metal screws at both ends of the cathode. Additional insulation and support were provided by ceramic balls placed near the mounting screws. Ceramic pieces lined the support structure to eliminate any line-of-sight path to the high voltage cathode. Ceramic paste was used to hold the ceramic pieces in place and fill any voids.

2.2. Basic chamber layout and operating conditions

The arrangement of the plasma processing system is shown in Fig. 2. The processing stages (or substrate holder) were introduced laterally, to the 'face' of the plasma sheet. Due to chamber layout(s), the stage was introduced at the middle of the 25×50 cm plasma sheets. Stage construction materials were similar to those used in the cathodes, with grounded support structures, r.f.-bias and temperature control capabilities. The diameter of the front electrode was approximately 13 cm. The electron beam was terminated at the chamber wall.

Experiments were carried out in a variety of vacuum chambers with the cathodes discussed previously. In every system, mass flow controllers were used for stable gas flow of 20–50 sccm and the high vacuum pump (turbomolecular or diffusion) was throttled with a manual valve or iris to set the operating pressure. All chambers were metal in construction and had base pressures below 2.6×10^{-4} Pa (2×10^{-6} Torr).

2.3. Reactive ion etching

Polymeric and semiconductor samples (approx. 1 cm^2) were mounted on the processing stage, which was positioned 1 cm from the e-beam edge. The processing stage was water cooled to keep the temperature at 20 ± 4 °C. In these tests, an r.f.-induced d.c. bias [7] level (bias voltage) was applied to the processing stage to vary the incident ion energies during the plasma pulse. Etch rates (ER) are determined through stylus profilometry (Tencor P-10) or scanning electron microscopy (SEM) analysis and are calculated from the total plasma exposure time and not the actual laboratory time.

Polymeric materials discussed in this work were industry standard negative or i-line photoresists and were etched in O_2/Ar gases. Fig. 3a shows the ER dependence for a negative resist as the bias voltage was varied. In these tests, plasmas were formed in 55 mTorr

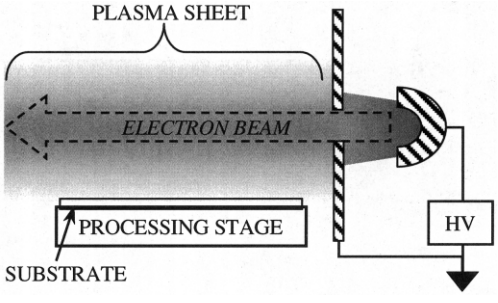

Fig. 2. Plasma processing arrangement using e-beam generated plasma.

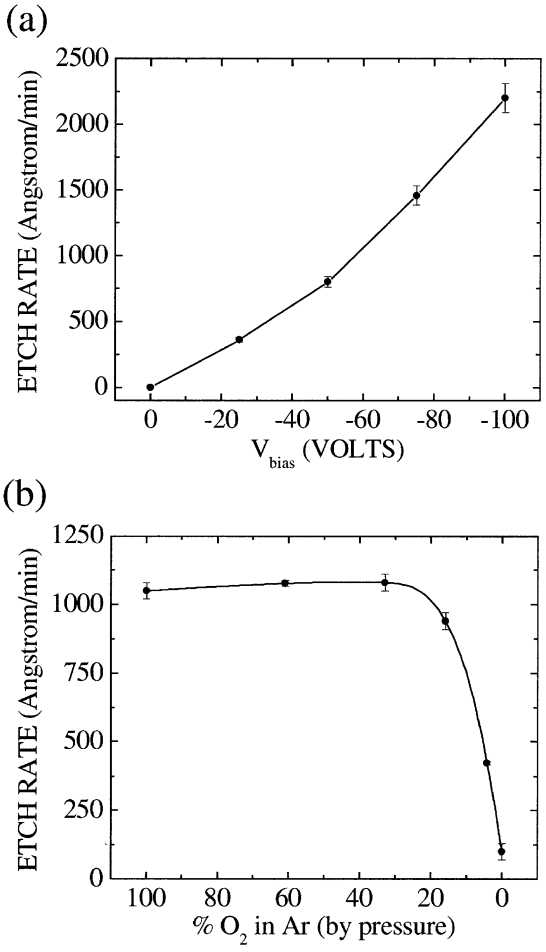

Fig. 3. Etch rates of negative photoresist material with respect to (a) bias voltage in pure O_2 and (b) percentage of O_2 at a fixed bias voltage of -50 V.

of pure oxygen. A moderately linear relationship between bias voltage and ER was seen, which increased strongly at higher voltages. Diluting the working gas with argon (keeping a fixed bias voltage of -50 V) resulted in the etch rate behavior shown in Fig. 3b. From this data, the ER remained fairly constant until the oxygen percentage dropped below 20%. It should be noted that the total gas pressure varied slightly in these experiments; the total pressure of the mixtures was $\sim$9 Pa (65 mTorr) but 7.3 Pa in pure O_2 and 10.6 Pa of Ar, respectively.

Fig. 4 shows the results from a feature cleaning test carried out in a pure O_2 plasma with a -50 V bias on the processing stage. The samples came from a commercial ashing process for Cu vias on i-line resist, shown by the SEM photo in Fig. 4a. This photo shows residual spires coming from around the edges of a 300 nm via, left behind after the [cleaning] ash process. The SEM photo in Fig. 4b shows removal of the residual spires after a 3-min e-beam plasma exposure.

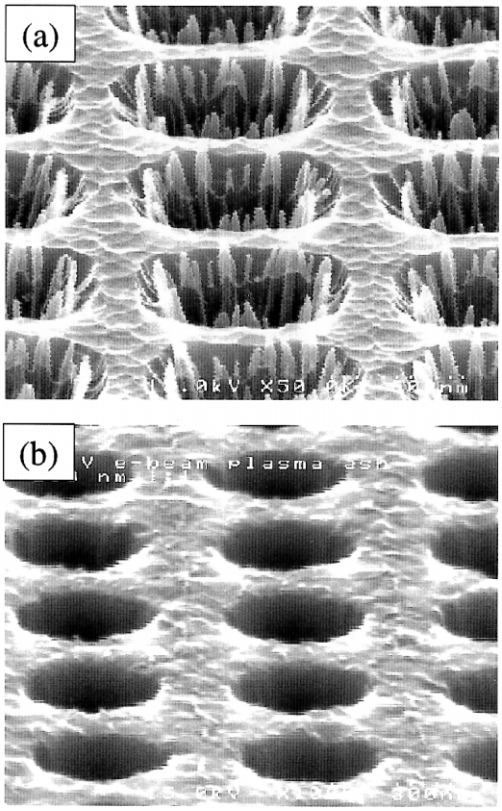

Fig. 4. Three hundred nanometers via structure (copper mask on top of i-line resist) (a) after standard industrial ash process and then (b) after a subsequent -50 V etch in e-beam produced O_2 plasma.

Similarly, mixtures of Ar or O_2 with SF_6 gas were used to etch crystalline $\langle 100 \rangle$ silicon. Fig. 5 shows the measured etch rates with respect to the bias voltage for O_2/SF_6 mixtures (55/8 sccm) and Ar/SF_6 mixtures (35/15 sccm). Operating pressures were $\sim$8 Pa and 9 Pa, respectively. The O_2 plasma shows an abrupt increase in ER at $V_{bias} = -200$ V, but was an order of

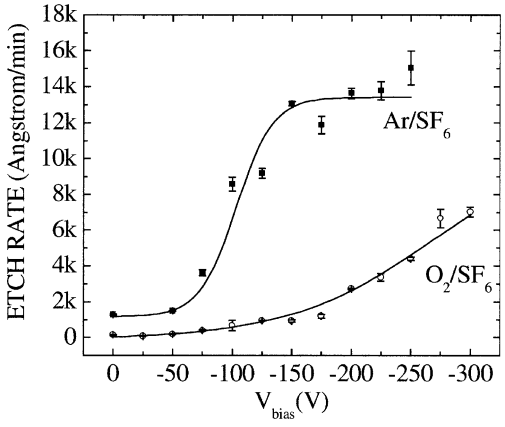

Fig. 5. Silicon etch rates with respect to bias voltage for O_2/SF_6 (55/8) and Ar/SF_6 (35/15) mixtures.

magnitude smaller than the Ar plasma for lower energies. The Ar plasma ER increased rapidly with a bias level above −50 V.

2.4. Plasma nitriding

These experiments are the subject of a recent article [8] so only minimal detail will be given here. Sample tiles, approximately 5×5 cm were cut from a 0.2-cm thick plate of 316 stainless steel. Each tile was polished to a surface roughness of 7 nm. Samples were then heated to 340–440 °C and cleaned in a Ar/H_2 plasma for 30 min before being exposed to a 60 mTorr N_2 plasma for 1.4 h of plasma exposure. A constant −100 V d.c. signal was applied to the processing stage for the cleaning and nitriding periods. Samples were allowed to cool, removed from vacuum and analyzed in the SEM to determine the surface nitride thickness. At 400 °C, a 1.3-μm thick layer was observed, increasing to 2.1 μm at 440 °C.

2.5. Diagnostics

Ion species were energy and mass resolved with a differentially pumped EQP300 Plasma Probe (Hiden Analytical Ltd.) as discussed in Ref. [4]. The sampling stage on the EQP was similar to the processing stages but electrically grounded and smaller in diameter (5.7 cm) with a 50 μm sampling orifice in the center. Relative ion fluxes in time at various analyzer energies are shown in Fig. 6 for a 3 ms plasma pulse with the sampling stage located 1 cm away from the e-beam of a 8 Pa nitrogen plasma.

The plasma densities and temperature were determined using a Langmuir probe, as discussed in Ref. [3]. Briefly, the body of the probe was constructed from alumina and stainless steel parts and contained a nichrome® wire heater to maintain a consistent probe surface [9]. The probe itself was a 250-μm diameter tungsten wire, which extended 0.2 cm from the ceramic housing. At the magnetic field strengths used (approx. 150 G) the plasma was not considered magnetized [10]. An iterative fit of the probe's current–voltage characteristic (up to the plasma potential) was used to determine the plasma density and temperature, not the electron saturation current. (These plasmas were also ambipolar, i.e. have equal electron and ion densities.) The analyzed data shown in Fig. 6c show steady-state primary plasma electron densities of 2×10^{11} cm^{-3} and temperatures of 0.4 eV for the nitrogen plasma discussed above.

3. Results and discussion

3.1. Electron beam generation and plasma production

Like any other hollow cathode source, these cathodes rely on plasma ions striking the inner wall and liberating

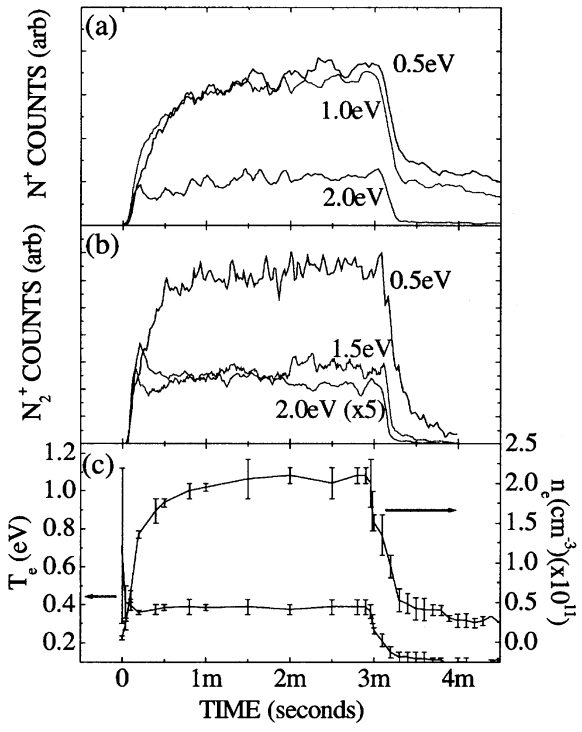

Fig. 6. Temporally resolved fluxes of (a) atomic and (b) molecular ions with fixed analyzer energies for a 60 mTorr N_2 plasma. (c) Plasma temperatures and densities at the center of the same N_2 plasma. Plasma pulse length was 3 ms.

secondary electrons. At typical (low) operating voltages, these secondary electrons are electrostatically accelerated away from cathode surface into the plasma where they quickly become thermalized through collisions with the background gas. The key to e-beam production in these pulsed hollow cathodes is the applied magnetic field and the parallel wall design of the cathode hollow slot.

Electrons emitted from the cathode sidewalls due to ion bombardment process around the applied magnetic field axis, with a gyroradius given (in centimeter) by $2.38[T_e\ (eV)]^{1/2}$ B (Gauss) [11]. These secondary electrons are a fraction (proportional to the cathode's secondary electron coefficient) of the hollow cathode plasma current and provide the electron beam. However, in the 150 G axial field, a secondary electron coming from the sidewall of the cathode hollow has a gyroradius comparable to the channel size (1 cm). These electrons can be trapped in the cathode producing a higher density plasma, which further enhances the ion flux to the surface. The actual beam electrons originate from the back wall, which will have the majority of their energy imparted parallel to the magnetic field. While an independent measurement of the e-beam current has not yet been made, the measured plasma densities and cathode operating currents suggest it was 10–100 $\mu A/cm^2$ in these experiments.

Plasmas produced by e-beams are quite different than conventional discharges. Their primary advantages for materials applications are (1) plasma production efficiency (discussed previously); (2) independence of plasma gas composition; (3) low temperature plasma electrons; and (4) scalability of these plasmas. The independence of the plasma production from gas composition also follows from the ionization efficiency of e-beams since the energy dependence of ionization cross sections is similar for all gases. Advantage (3), low electron temperatures (and internal fields) are due to the fact that plasma electrons are merely a by-product of the e-beam ionization process and the plasma sustenance is not driven by the final plasma electron distribution. These points are all illustrated in Fig. 6, which shows extremely low electron temperatures and subsequent ion energies for a high density plasma (note also the rapid steady-state condition in the Fig. 6 data). Finally, from the design considerations given here, it should be clear that the width of an e-beam could be extended indefinitely, at least to the current limit of the cathode power supply. In our lab, we have indeed extended the e-beam to 50-cm wide and still operate well within the range of commercial 2–5 kV power supplies.

3.2. Applications

The experiments discussed here were pulsed due to an earlier design (based on a different application as discussed in Ref. [1] and were intended to be proof-of-concept tests for the practicality of applying e-beam produced plasmas to more widespread applications. Although not the focus of this paper, modulated plasmas offer advantages in process space [12] not always accessible with continuous plasma sources. In order to take full advantage of the versatility of these plasma sources, a more comprehensive design-of-experiments is necessary to optimize the processes.

The reactive ion etching of polymer materials shows strong promise in terms of precise control of a typically isotropic, uncontrollable process that relies strongly on the desorption of carbon monoxide (CO) from the surface. From the data shown in Figs. 3 and 4, etching of the resist material in these experiments was an ion-driven process in an environment that contained an abundance of atomic oxygen neutrals. The direct correlation between ion energy and material removal in Fig. 3 shows that some ion energy was in fact necessary to remove material and the removal was not automatic (exothermic) in the presence of atomic oxygen, since the ER drops to nearly zero with no bias energy. In other plasma sources, organic material removal is considered a chemical process dependent only on the atomic oxygen flux to the surface. Thus, ion energy is not considered important in sources where the plasma potential exceeds 10 V. However, plasma potentials in e-beam produced plasmas are only 1–5 V, so initial ion energies are greatly reduced. Without some sort of additional activation (ion energy, temperature) the desorption of volatile etch species does not progress at measurable rates. This control of ion energy down to extremely low energies provides additional benefits, as shown by the via residue removal in Fig. 4. These test structures provided a much more rigorous test for process anisotropy and showed submicron feature evolution in an otherwise isotropic process. With only very fine (approx. 50 nm) residues within small features, any process isotropy would quickly destroy the feature profile. Instead, a clean removal of the residuals left behind was seen, leaving the via structure intact. The results of Fig. 3b suggests the plasma source produced a large reactive neutral flux, as the ER remained constant while the feedstock gas source of atomic oxygen was reduced. The ER was, therefore, not neutral-limited, until the molecular gas percentage fell below 20%.

The reactive ion etching of silicon also showed promising results in terms of material removal rates. For the Ar/SF_6 mixtures, an ER of $\sim 1\ \mu m/min$ at moderate bias voltages (-125 V) was shown in Fig. 5. Although the amount of SF_6 was lower in the O_2/SF_6 plasmas, the order of magnitude difference in ER at low energies was surprising. This lower ER is more indicative of a SiO_2 sputter yield at these energies, which is reasonable for the more dilute SF_6 plasmas. The flux of etchants was dominated by oxidizing species, causing the surface to become more like SiO_2 than the bulk silicon prior to etching. In addition, the selectivity of SiO_2 over Si using SF_6 at these ion energies should be appreciable, although preliminary tests using an SiO_2 mask showed no selectivity in this plasma chemistry further suggesting SiO_x removal as the limiting step. The Ar/SF_6 plasma chemistry conversely showed a strong reactive ion etch component, removing material much more rapidly than sputtering alone and leveling out at the -200 V energy threshold.

While the plasma nitriding experiments require further composition analysis, the results are encouraging for a non-optimized plasma process. The growth rates are comparable with standard techniques using r.f. and d.c. glow discharges (see Ref. [8] and the references therein). Moreover, the nitrogen plasmas produce large fluxes of atomic nitrogen ions and neutrals, analogous to the oxygen plasmas discussed earlier. With the additional kinetic energy from the applied d.c. voltage, the atomic ions are the likely critical species for this process, considering that it is atomic nitrogen that adsorbs and diffuses into the bulk. The fact that e-beam produced plasmas in diatomic gases supply predominantly atomic [4] ions to the workpiece from makes it an attractive system for plasma nitriding of materials.

4. Conclusion

Electron-beam produced plasmas were readily produced and used in various materials processing applications. These plasma sources offer considerable flexibility for modifying materials, although only a few of the attributes have been investigated thus far. The absence of high plasma electron temperatures (and, therefore, large plasma potentials) allows a variety of processing conditions without sacrificing flux of reactive charged or neutral species. This work demonstrated important attributes of ion energy control and damage-free etching possibilities, versatility of gas compositions, competitive nitriding rates and scalability within an actual plasma-processing environment.

Acknowledgments

The authors gratefully appreciate the assistance of Dr John Hallock (formerly of Axcelis Technologies, Rockville, MD) with the via structures. The technical assistance of Anthony Noll (NRL) and Robert Lanham (SFA, Inc., Lanham, MD) was also greatly appreciated. The Office of Naval Research supported this work.

References

[1] R.F. Fernsler, W.M. Manheimer, R.A. Meger, J. Mathew, D.P. Murphy, R.E. Pechacek, et al., Phys. Plasmas 5 (1998) 2137.

[2] W.M. Manheimer, R.F. Fernsler, M. Lampe, R.A. Meger, Plasma Sources Sci. Technol. 9 (2000) 370.

[3] D. Leonhardt, S.G. Walton, D.D. Blackwell, W.E. Amatucci, D.P. Murphy, R.F. Fernsler, et al., J. Vac. Sci. Technol. A 19 (2001) 1367.

[4] S.G. Walton, D. Leonhardt, D.D. Blackwell, D.P. Murphy, R.F. Fernsler, R.A. Meger, J. Vac. Sci. Technol. A 19 (2001) 1325.

[5] D. Leonhardt, Vac. Technol. Coat. 24 (November 2001).

[6] It should be noted that previous versions of these cathodes made of brass with Telfon® insulation performed similarly. The use of these robust and vacuum compatible materials greatly enhanced the operation lifetime and versatility of the cathode.

[7] R. Patrick, S. Baldwin, N. Williams, J. Vac. Sci. Technol. A 18 (2000) 405.

[8] C. Muratore, D. Leonhardt, S.G. Walton, D.D. Blackwell, R.F. Fernsler, R.A. Meger, submitted to Surf. Coat. Technol..

[9] W.E. Amatucci, P.W. Schuck, D.N. Walker, P.M. Kinter, S. Powell, B. Holback, et al., Rev. Sci. Instrum. 72 (2001) 2052.

[10] Magnetized plasmas demonstrate a skewed electron saturation current due to a depletion of the magnetic flux tube that intersects the Langmuir probe, although other plasma parameters are relatively unchanged. See B.-W. Koo, N. Hershkowitz, J. Appl. Phys. 86 (1999) 1213.

[11] J.D. Huba, NRL Plasma Formulary (NRL/PU/6790—00-426), Naval Research Laboratory, Washington, DC (2000). It should be noted that T_e is the component of the electron temperature perpendicular to the magnetic field.

[12] L. Bárdoš, H. Baránková, Vac. Technol. Coat. 47 (September 2001).